



HAL
open science

A neuropathological study of cerebrovascular abnormalities in a signal transducer and activator of transcription 3-deficient patient

Marie-Olivia Chandesris, Françoise Gray, Patrick Bruneval, Arshid Azarine, Nathalie Boddaert, Catherine Oppenheim, François Paraire, Emmanuel Touzé, Damien Bonnet, Olivier Hermine, et al.

► To cite this version:

Marie-Olivia Chandesris, Françoise Gray, Patrick Bruneval, Arshid Azarine, Nathalie Boddaert, et al.. A neuropathological study of cerebrovascular abnormalities in a signal transducer and activator of transcription 3-deficient patient. *Journal of Allergy and Clinical Immunology*, 2015, 136 (5), pp.1418-1421.e5. 10.1016/j.jaci.2015.05.021 . hal-04331812

HAL Id: hal-04331812

<https://hal.science/hal-04331812>

Submitted on 15 Dec 2023

HAL is a multi-disciplinary open access archive for the deposit and dissemination of scientific research documents, whether they are published or not. The documents may come from teaching and research institutions in France or abroad, or from public or private research centers.

L'archive ouverte pluridisciplinaire **HAL**, est destinée au dépôt et à la diffusion de documents scientifiques de niveau recherche, publiés ou non, émanant des établissements d'enseignement et de recherche français ou étrangers, des laboratoires publics ou privés.



Distributed under a Creative Commons Attribution - NonCommercial - NoDerivatives 4.0 International License

ImmunoCAP results as being sensitized to wheat flour. These subjects would not have had to undergo invasive SICTs, which are not without risk, to confirm the diagnosis because a positive result with the recombinant allergens added to clinical complaints would have allowed us to make the diagnosis. We assume that adding further recombinant allergens described in the literature⁴ would allow us to identify additional bakers sensitized to wheat flour. Accurate diagnosis and identification of the relevant allergens might have important health and economic consequences for patients with baker's asthma.

We thank Marcial Velasco Garrido for valuable input to the manuscript.

Cordula Bittner, MD^a
Ulrike Peters, BTA^c
Karsten Frenzel, PhD^c
Horst Müsken, MD^b
Reinhold Bretschneider, PhD^c

From ^athe Institute of Occupational Medicine and Maritime Medicine (ZfAM), University Medical Center Hamburg-Eppendorf, Hamburg, Germany; ^bPractice Müsken, Bad Lippspringe, Germany; and ^cBiocenter Klein Flottbek and Botanical Garden, University of Hamburg, Hamburg, Germany. E-mail: cordula.bittner@bgv.hamburg.de.

Supported in part by Deutsche Forschungsgemeinschaft, Bonn, Germany (grant BI 812/1-1).

Disclosure of potential conflict of interest: C. Bittner has received research support from Deutsche Forschungsgemeinschaft (grant BI 812/1-1). The rest of the authors declare that they have no relevant conflicts of interest.

REFERENCES

1. Brisman J. Baker's asthma. *Occup Environ Med* 2002;59:498-502.
2. Olivieri M, Biscardo CA, Palazzo P, Pahr S, Malerba G, Ferrara R, et al. Wheat IgE profiling and wheat IgE levels in bakers with allergic occupational phenotypes. *Occup Environ Med* 2013;70:617-22.
3. Wisniewska M, Nowakowska-Swirta E, Palczynski C, Walusiak-Skorupa J. Diagnosing of bakers' respiratory allergy: is specific inhalation challenge test essential? *Allergy Asthma Proc* 2011;32:111-8.
4. Sander I, Rozynek P, Rihs HP, van Kampen V, Chew FT, Lee WS, et al. Multiple wheat flour allergens and cross-reactive carbohydrate determinants bind IgE in baker's asthma. *Allergy* 2011;66:1208-15.
5. Pahr S, Constantin C, Mari A, Scheibhofer S, Thalhamer J, Ebner C, et al. Molecular characterization of wheat allergens specifically recognized by patients suffering from wheat-induced respiratory allergy. *Clin Exp Allergy* 2012;42:597-609.
6. Bittner C, Grassau B, Frenzel K, Baur X. Identification of wheat gliadins as an allergen family related to baker's asthma. *J Allergy Clin Immunol* 2008;121:744-9.
7. Cramer R, Achatz G, Weichel M, Rhyner C. Direct selection of cDNAs by phage display. *Methods Mol Biol* 2002;185:461-9.

Available online June 19, 2015.

<http://dx.doi.org/10.1016/j.jaci.2015.05.010>

A neuropathological study of cerebrovascular abnormalities in a signal transducer and activator of transcription 3-deficient patient

To the Editor:

Human signal transducer and activator of transcription 3 (STAT3) deficiency (Online Mendelian Inheritance in Man [OMIM] no. 147060) is a rare primary immunodeficiency caused by heterozygous mutations of *STAT3*, conferring susceptibility to infections and skeletal and connective tissues features. Recent morphologic data revealed that STAT3 deficiency is responsible for a diffuse vasculopathy,¹⁻⁴ which is characterized by alteration in mechanotransduction in the arterial wall causing hypotrophic remodeling despite increased forces exerting on the wall (circumferential wall stress), leading to enhanced susceptibility to aneurysm.

The high vascular risk of such lesions was confirmed by the sudden death of a 35-year-old patient (carrying a missense F384L *STAT3* mutation) after rupture of a giant basilar artery aneurysm (see Fig E1 in this article's Online Repository at

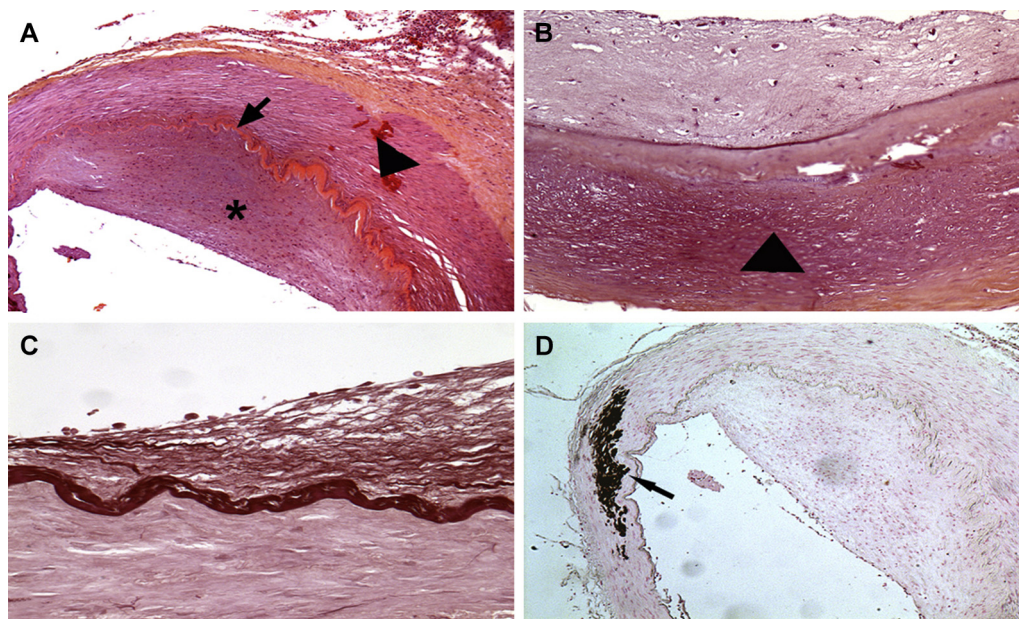


FIG 1. Microscopic analysis of the basilar trunk. **A**, Preserved media (arrowhead), irregular thickening of the internal elastic lamina (arrow), and focal intimal hyperplasia (asterisk) in the nonaneurysmal part of the artery (hematoxylin and eosin). **B**, Fibrosis and complete loss of VSMCs in the media (arrowhead) in the aneurysmal part of the artery (hematoxylin and eosin). **C**, Thickening of the internal elastic lamina highlighted by elastic stain. **D**, Massive calcification (arrow) of media (von Kossa stain).

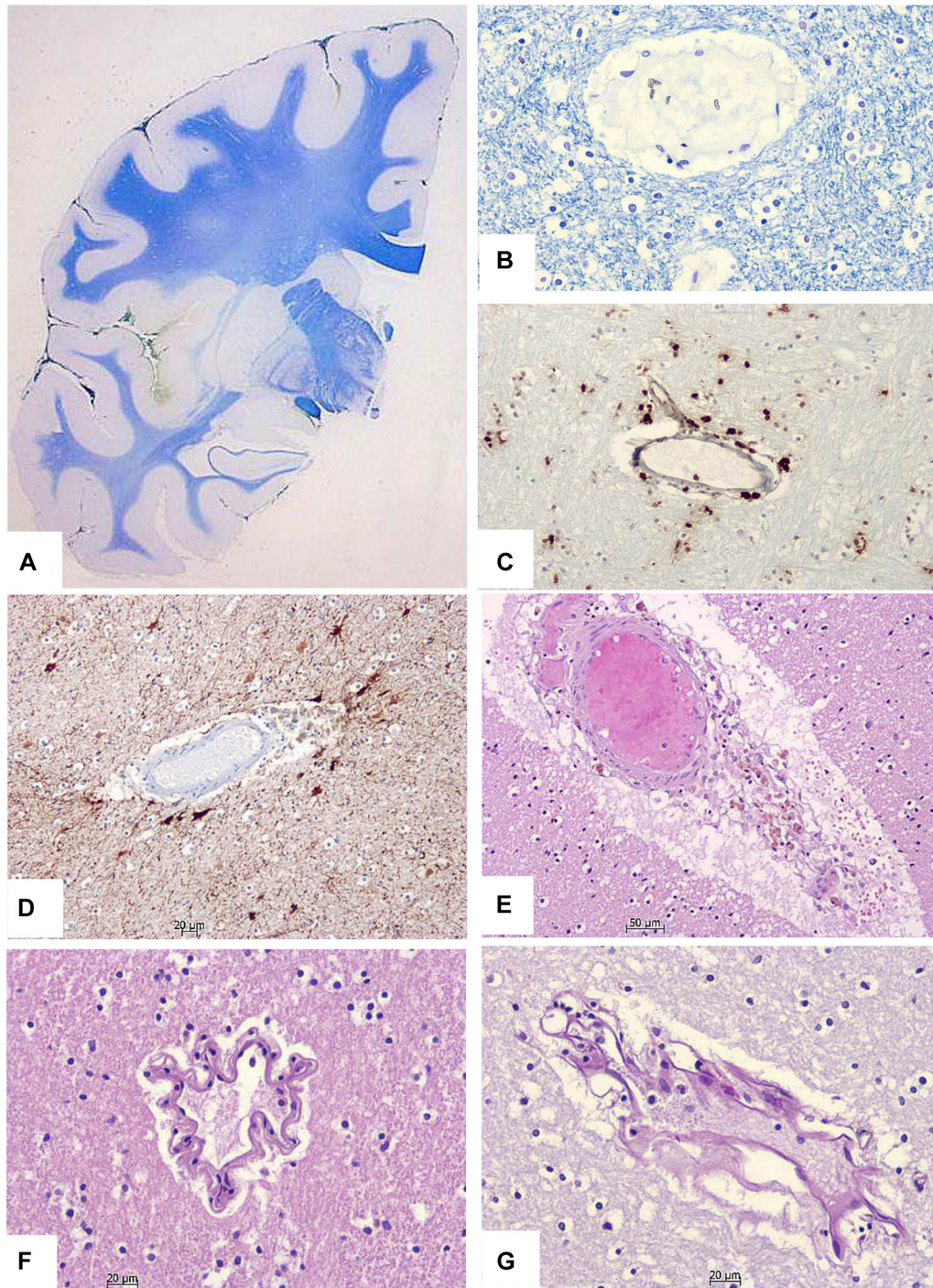


FIG 2. White matter and intracerebral small-vessel disease. **A**, Coronal section of the right cerebral hemisphere (Klüver and Barrera stain) revealing mild and ill-delimited myelin pallor in the deep white matter. **B**, Spongiosis and oligodendroglial tumefaction (Klüver and Barrera stain). **C**, Microglial activation (anti-CD68 staining). **D**, Astrocytic gliosis (glial fibrillary acidic protein). **E**, Dilatation of the perivascular spaces with plasma exudate and accumulation of macrophages containing brownish pigment (hematoxylin and eosin). **F** and **G**, Convuluted and frizzy-like aspect of the small-vessel wall (Fig 2, *F*, hematoxylin and eosin; Fig 2, *G*, periodic acid-Schiff).

www.jacionline.org). After consent of his family, an autopsy was performed 24 hours after death.

We report on the neuropathological study of the brain. The materials and methods used in this study are detailed in

the [Methods](http://www.jacionline.org) section in this article's Online Repository at www.jacionline.org. Macroscopic analysis confirmed that aneurysmal rupture led to abundant bleeding, intracranial hypertension, and fatal tonsillar herniation. The white matter

appeared grayish in areas where white matter hyperintensities had been observed in magnetic resonance imaging. Microscopy revealed damage of both blood vessels and white matter.

The aneurysmal wall (Fig 1) presented marked thickness variations of the intima with focal intimal hyperplasia and of the media with loss of vascular smooth muscle cells (VSMCs) in atrophic areas. The internal elastic lamina exhibited major irregularities with either focal thickening or disruption in areas with marked VSMC loss. Medial calcifications were observed as either thin deposits along the internal elastic lamina or massive aggregates. The absence of lipids and inflammation in the aneurysmal wall or the other cerebral vessels ruled out atherosclerosis and vasculitis as causes.

The large vessels (basilar, vertebral, and carotid arteries; see Fig E2 in this article's Online Repository at www.jacionline.org) appeared flattened, with thinned walls, marked fibrosis of the media, focal endothelial hyperplasia, and an abnormal thick, irregular, disrupted internal elastic membrane containing alcianophilic (mucopolysaccharide) deposits. There were also focal calcium deposits affecting all 3 layers of the vessel wall. Apart from the calcifications, the abnormalities observed in the small and medium arteries (Willis circle and middle and anterior cerebral arteries) were similar to those of large vessels.

In agreement with magnetic resonance imaging data, white matter changes (Fig 2) were mild and limited in extent, affecting the deep white matter in the parieto-occipital and fronto-orbital regions. They included spongiosis, oligodendroglial tumefaction, dilation of the perivascular spaces with plasma exudate, pigment-laden macrophages, signs of microglial activation, and astrocytic gliosis. These features, which were consistent with chronic edema and involvement of the blood-brain barrier, were associated with an abnormal convoluted and frizzy aspect of the vascular wall. In immunohistochemistry CD3 lymphocytes and CD68 macrophages were scarce, confirming the absence of inflammation.

The medial VSMCs of the basilar aneurysm expressed higher levels of TGF- β than in healthy control arteries, but no difference was detected in phospho-SMAD2 expression (see Fig E3 in this article's Online Repository at www.jacionline.org). Although all vascular cells showed STAT3 expression, phospho-STAT3 staining was negative in medial VSMCs of the basilar aneurysm and was reduced in the patient's nonaneurysmal cerebral and peripheral arteries compared with strong positive staining in healthy control arteries.

This neuropathological analysis provides insights into the nature of the vascular lesions observed in patients with STAT3 deficiency. It decisively rules out atherosclerosis, inflammatory mechanisms, and/or infectious disease and reveals lesions that had never been described before. The association of vascular lesions with white matter changes similar to those seen in patients with chronic vascular leukoencephalopathy prompted us to suggest an exclusively vascular noninflammatory mechanism combining ischemia and chronic edema. However, it is noteworthy that conditional Stat3 deficiency in murine astrocytes is associated with exacerbated white matter injuries,⁵ suggesting that alterations in STAT3 signaling in nonvascular cells might also contribute to white matter abnormalities. The present morphologic and histologic characteristics are somewhat reminiscent of other genetic connective tissue diseases associated with an increased risk of cardiovascular complications, including aneurysm formation (see Table E1 in this article's Online

Repository at www.jacionline.org). However, their pathophysiological link remains hypothetical.

Pseudoxanthoma elasticum (OMIM no. 264800), which is caused by autosomal recessive mutations in *ABCC6* coding for an ATP-binding protein, is characterized by elastocalcinosis (resulting in elastic fiber fragmentation) and proteoglycan accumulation in soft conjunctive tissues and the arterial media.⁶ The arterial lesions consist of mineralization of the elastic fibers within the media of small- and medium-caliber musculoelastic arteries associated with abnormal extracellular matrix remodeling (proteoglycan replacement and activation of matrix metalloproteinases). However, the VSMCs appear to be normal, and the arterial elasticity is either unchanged or increased. The link between these 2 conditions remains hypothetical because the *ABCC6* gene product's putative biological functions and substrates are unknown and a relationship with STAT3 has not been demonstrated.

Williams-Beuren syndrome (OMIM no. 194050) is a genetic multisystem disease related to deletion of genes on chromosome 7q11.23, including *ELN*, which encodes for elastin.⁷ The main pathological feature consists of VSMC overgrowth toward the lumen with wall expansion responsible for a systemic obstructive arteriopathy. Apart from the common alteration in elastic fibers, the other pathological features are not observed in the STAT3-deficient patient. Moreover, interaction between STAT3 and elastin has never been reported.

Marfan syndrome (OMIM no. 154700) is caused by mutations in *FBNI*, encoding fibrillin 1, the main component of the extracellular matrix microfibril present in all tissues.⁸ The main pathological features include low elastin content, calcifications and fragmentation of elastic fibers, vascular wall inflammation, intimal hyperplasia (caused by VSMC overgrowth), and structural collapse of the vessel wall resulting in aortic root aneurysm with high risk of dissection and valve disease. In this respect it is noteworthy that conditional deletion of *Stat3* in murine astrocytes is associated with enhanced production of TGF- β ,⁵ as is the case in syndromic and nonsyndromic aneurysms.⁹ This putative link between STAT3- and TGF- β -related aneurysms is worth further investigation.

In conclusion, this is the first detailed report on a unique and previously uncharacterized vasculopathy associated with STAT3 deficiency. The fact that this vascular phenotype has some features in common with other multisystem genetic connective tissue diseases reinforces the hypothesis of a common underlying mechanism. Further investigation of this hypothesis might provide important insights into new potential treatments for connective tissue diseases. In the meanwhile, strict control of vascular risk factors (smoking, overweight, and hypertension) that might accelerate disease progression is necessary.

Marie-Olivia Chandesris, MD^{a,b,c}

Françoise Gray, MD, PhD^d

Patrick Bruneval, MD^{b,e}

Arshid Azarine, MD^{b,f}

Nathalie Boddaert, MD, PhD^{b,g}

Catherine Oppenheim, MD, PhD^{b,h,i}

François Paraire, MD^j

Emmanuel Touzé, MD, PhD^{b,k,l}

Damien Bonnet, MD, PhD^{b,m}

Olivier Hermine, MD, PhD^{a,b,c,n}

Olivier Lortholary, MD, PhD^{b,c,o,p,q}

Valérie Cormier-Daire, MD, PhD^{b,n,r}

Pierre Boutouyrie, MD, PhD^{b,s,t}

Ziad Mallat, PhD^{b,t,u}
Alain Fischer, MD, PhD^{b,c,n,v,w}
Capucine Picard, MD, PhD^{b,c,x,y}

From ^athe Department of Haematology, Necker Children's Hospital, ^cCentre de référence des déficits immunitaires héréditaires (CEREDIH), ^sthe Department of Paediatric Radiology, ^mM3C Centre de Référence pour les Malformations Cardiaques Congénitales Complexes, Department of Paediatric Cardiology, ^tthe Department of Genetics, ^vthe Paediatric Immunohematology Unit, and ^wthe Study Centre for Primary Immunodeficiencies, Necker Children's Hospital, Assistance Publique-Hôpitaux de Paris (APHP), Paris, France; ^bSorbonne Paris Cité, Paris Descartes University, Imagine Institute, Paris, France; ^dthe Department of Pathology (Neuropathology), Lariboisière Hospital, APHP, Paris 7 University, Paris, France; ^ethe Department of Pathology, ^fthe Department of Radiology, and ^gthe Pharmacology Department, Georges Pompidou European Hospital, APHP, Paris, France; ^hthe Department of Neuroradiology, Sainte-Anne Hospital, Paris, France; ⁱINSERM UMR 894, Paris, France; ^jthe Department of Forensic Medicine and Pathology, Raymond Poincaré Hospital, APHP, Versailles Saint-Quentin-en-Yvelines University, Garches, France; ^kthe Department of Neurology, Sainte-Anne Hospital, Paris, France; ^lUniversity of Caen Basse-Normandie, Côte de Nacre Hospital, Caen, France; ⁿINSERM UMR 1163, IMAGINE Institut, Paris, France; ^othe Department of Infectious Diseases and Tropical Medicine, Necker Children's Hospital, APHP, Paris, France; ^pPasteur Institute, Paris, France; ^qCNRS URA3012, Paris, France; ^rINSERM U970, Paris-Cardiovascular Research Centre (PARCC), Paris, France; ^uthe Division of Cardiovascular Medicine, Addenbrooke's Hospital, University of Cambridge, Cambridge, United Kingdom; ^wCollege de France, Paris, France; and ^ythe Laboratory of Human Genetics of Infectious Diseases, Necker Branch, INSERM UMR 1163, IMAGINE Institute, Paris, France. E-mail: olivia.chandesris@nck.aphp.fr.

Disclosure of potential conflict of interest: E. Touzé is a board member for BMS, Pfizer, Boehringer Ingelheim, and Bayer and has received payment for lectures from Boehringer Ingelheim, Pfizer, Bayer, and BMS. O. Hermine is a board member for, has consultant arrangements with, and receives stock/stock options from AB Science; has received research support from Celgene and Novartis; and has received payment

for lectures from Jansen and Celgene. O. Lortholary is a board member for MSD, has consultant arrangements with Gilead, and has received payment for lectures from Pfizer, Astellas, Gilead, Merck, and Schering. A. Fischer has received research support from the European Research Council ("PIDIMMUN" Grant no. 249816). The rest of the authors declare that they have no relevant conflicts of interest.

REFERENCES

1. Ling JC, Freeman AF, Gharib AM, Arai AE, Lederman RJ, Rosing DR, et al. Coronary artery aneurysms in patients with hyper IgE recurrent infection syndrome. *Clin Immunol* 2007;122:255-8.
2. Gharib AM, Pettigrew RI, Elagha A, Hsu A, Welch P, Holland SM, et al. Coronary abnormalities in hyper-IgE recurrent infection syndrome: depiction at coronary MDCT angiography. *AJR Am J Roentgenol* 2009;193:W478-81.
3. Freeman AF, Avila EM, Shaw PA, Davis J, Hsu AP, Welch P, et al. Coronary artery abnormalities in hyper-IgE syndrome. *J Clin Immunol* 2011;31:338-45.
4. Chandesris MO, Azarine A, Ong KT, Taleb S, Boutouyrie P, Mousseaux E, et al. Frequent and widespread vascular abnormalities in human signal transducer and activator of transcription 3 deficiency. *Circ Cardiovasc Genet* 2012;5:25-34.
5. Nobuta H, Ghiani CA, Paez PM, Spreuer V, Dong H, Korsak RA, et al. STAT3-mediated astrogliosis protects myelin development in neonatal brain injury. *Ann Neurol* 2012;72:750-65.
6. Leftheriotis G, Omarjee L, Le Saux O, Henrion D, Abraham P, Prunier F, et al. The vascular phenotype in Pseudoxanthoma elasticum and related disorders: contribution of a genetic disease to the understanding of vascular calcification. *Front Genet* 2013;4:4.
7. Pober BR. Williams-Beuren syndrome. *N Engl J Med* 2010;362:239-52.
8. Judge DP, Dietz HC. Marfan's syndrome. *Lancet* 2005;366:1965-76.
9. Gomez D, Al Haj Zen A, Borges LF, Philippe M, Gutierrez PS, Jondeau G, et al. Syndromic and non-syndromic aneurysms of the human ascending aorta share activation of the Smad2 pathway. *J Pathol* 2009;218:131-42.

Available online June 30, 2015.
<http://dx.doi.org/10.1016/j.jaci.2015.05.021>

METHODS

Autopsy was performed 24 hours after death. Gross examination of the formalin-fixed brain was performed on coronal sections of the cerebral hemispheres and sections of the brain stem and cerebellum perpendicular to their axis. Large coronal slices of the cerebral hemispheres were embedded in paraffin, and 15- μ m-thick sections were stained with hematoxylin and eosin and a combination of cresyl violet and Luxol fast blue (Klüver and Barrera stain). Smaller blocks were taken from the cerebral vessels, aneurysm, cerebral cortex with underlying white matter, deep white matter, deep gray nuclei, midbrain, cerebellum, and brainstem and then embedded in paraffin. Five-micrometer-thick sections were stained with hematoxylin and eosin, cresyl violet, Masson trichrome, periodic acid-Schiff, Bodian silver impregnation combined with Luxol fast blue, alcian blue, orcein elastin stain (to highlight elastic fibers), and von Kossa stain (to highlight calcium deposits).

An immunohistochemical analysis was performed on selected samples from frontal and occipital white matter, cerebral vessels, and the aneurysm by using either a Roche Diagnostic (Mannheim, Germany) automat for routine antibodies (CD3, CD68, and glial fibrillary acidic protein) or a manual technique for the other specific antibodies (with an avidin-biotin complex and peroxidase [Vector Laboratories, Burlingame, Calif]). Specific primary antibodies against the following antigens were used: CD3 (for T lymphocytes), CD68 (for macrophages), glial fibrillary acidic protein (for astrocytes; all from Dako Cytomation, Glostrup, Denmark), STAT3, phospho-STAT3, phospho-SMAD2 (all from Cell Signaling, Danvers, Mass), and TGF- β (AbD Serotec, Raleigh, NC). In negative controls specific primary antibodies were replaced by nonrelevant mouse or rabbit antibodies. The immunohistochemical data for the basilar trunk were compared with those for a normal popliteal artery section (obtained during femoral-popliteal bypass surgery).

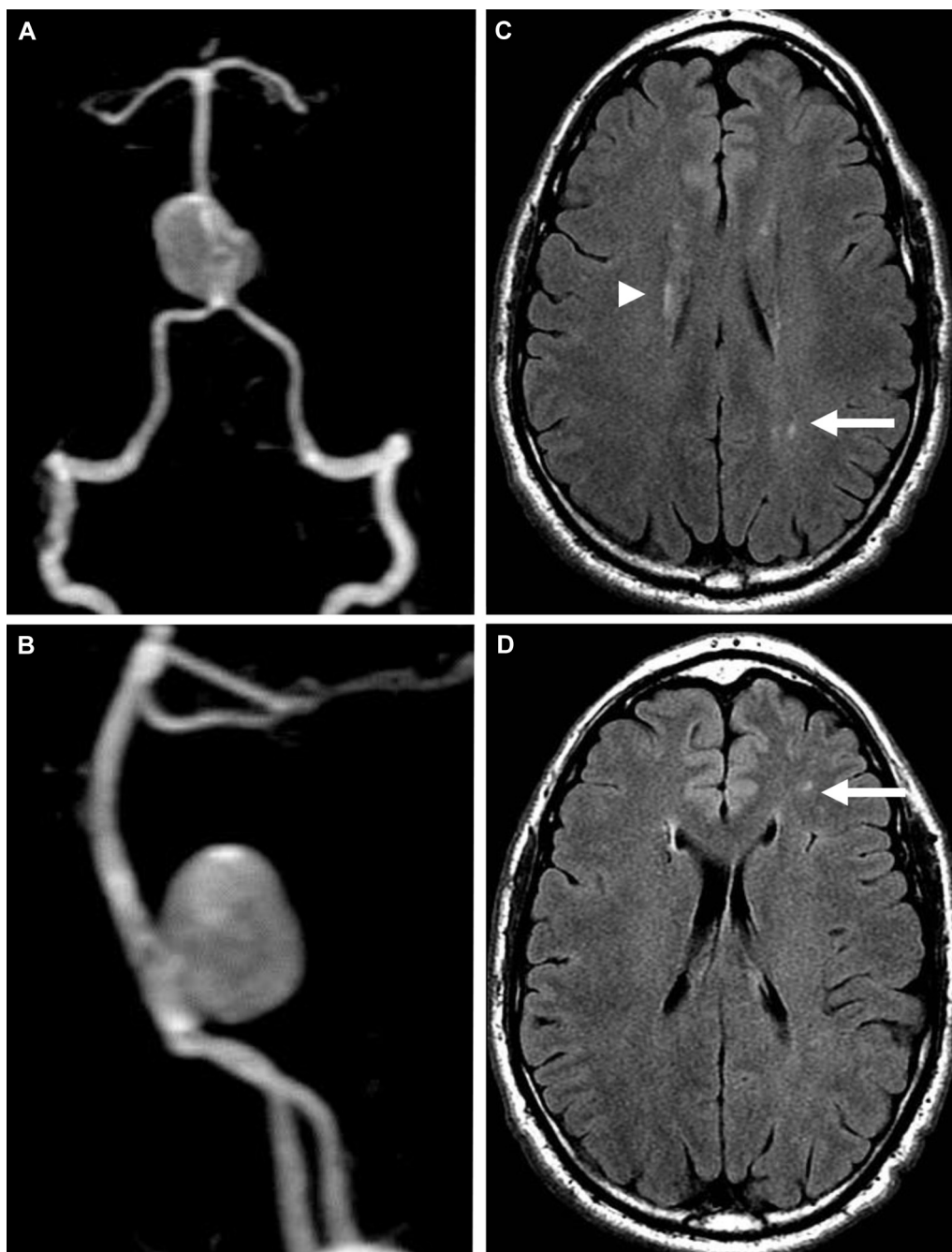


FIG E1. Brain magnetic resonance imaging (3-Tesla magnetic resonance imaging) findings. **A** and **B**, Three-dimensional reconstruction of contrast-enhanced magnetic resonance angiographic data, revealing a 19.5 × 17-mm saccular aneurysm of the basilar artery. **C** and **D**, Axial fluid-attenuated inversion recovery images demonstrating the presence of white matter hyperintensities (*arrow*) and linear periventricular hyperintensities (*arrowhead*).

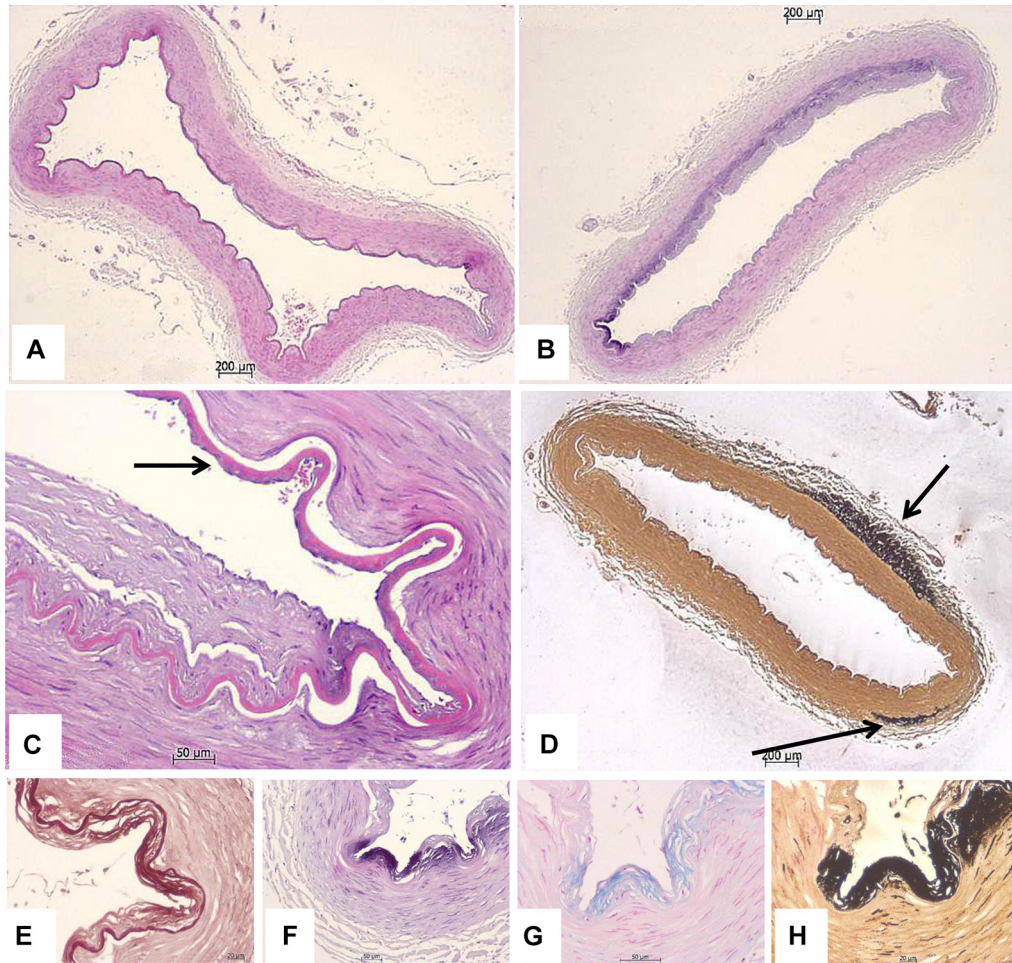


FIG E2. Microscopic appearance of the arteries in the circle of Willis. **A**, Full section of the basilar artery (hematoxylin and eosin stain). The vessel appears somewhat flattened, with a thin wall. **B**, Full section of the right vertebral artery (hematoxylin and eosin stain). Again, the vessel appears somewhat flattened, with a thin wall. Note the basophilic calcium deposits in the media and (focally) intima. **C**, Left middle cerebral artery (hematoxylin and eosin stain) showing focal endothelial hyperplasia. Note the eosinophilic deposits under the intima (*arrow*). **D**, Full section of the left vertebral artery section (von Kossa stain). The vessel appears somewhat flattened, with a thin wall. Note the calcium deposits (stained black with the von Kossa technique) in the adventitia (*arrows*). **E-H**, Right vertebral artery (Fig E2, *E*, orcein stain for elastin; Fig E2, *F*, hematoxylin and eosin stain; Fig E2, *G*, alcian blue stain; and Fig E2, *H*, von Kossa stain). The internal elastic membrane shows abnormal thickening, irregularities and disruptions (Fig E2, *E*) associated with alcianophilic (mucopolysaccharide) deposits (Fig E2, *G*) and basophilic (Fig E2, *F*) von Kossa-positive (Fig E2, *H*) calcium deposits.

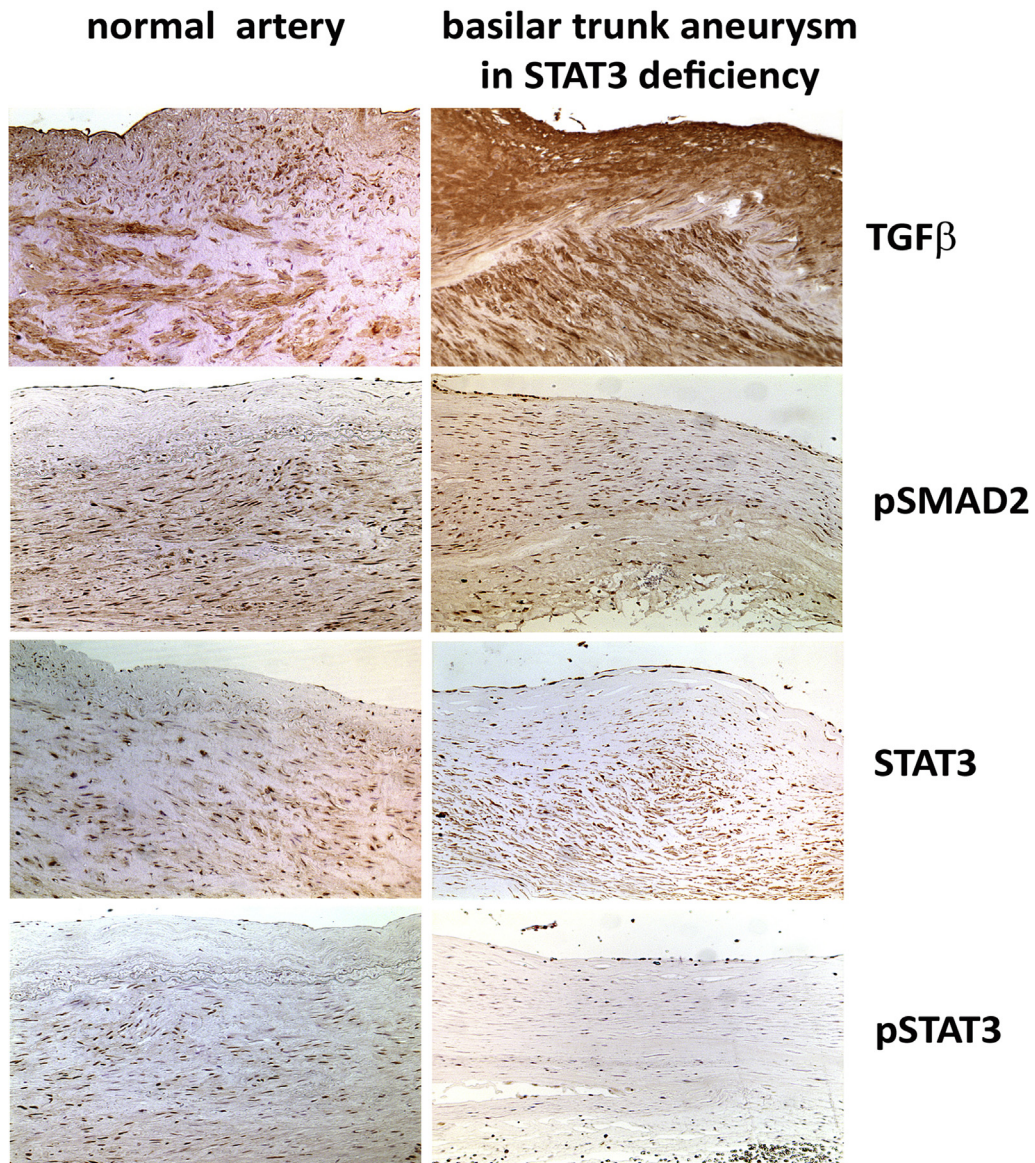


FIG E3. Expression levels of TGF- β , phospho-SMAD2, STAT3, and phospho-STAT3 in VSMCs from a normal (control) artery and from the basilar artery aneurysm. TGF- β expression was higher in the aneurysm than in the normal artery. No difference was observed for phospho-SMAD2. Although both the control artery and basilar aneurysm artery expressed similar levels of STAT3, phospho-STAT3 was differentially expressed. The VSMCs in the basilar artery aneurysm did not express phospho-STAT3, whereas the protein was strongly expressed in the normal (control) artery. Immunohistochemistry was performed with specific primary antibodies (original magnification $\times 10$).

TABLE E1. Comparative analysis of STAT3 deficiency-related vasculopathy with the vasculopathy of 3 relevant genetic connective tissue diseases

	AD-HIES	Pseudoxanthoma elasticum	Williams-Beuren syndrome	Marfan syndrome
Gene	<i>STAT3</i>	<i>ABCC6</i>	<i>ELN</i>	<i>FBNI</i>
Size of involved vessels	Large/medium/small	Medium/small	Large/medium	Large/medium
Aneurysm	Yes	Yes	No	Yes
Stenosis	Yes	Yes	Yes (severe)	No
Cerebral parenchyma (MRI)	Leukoencephalopathy, strokes, atrophy	Strokes	Atrophy, strokes	Strokes
IMT	Decreased (despite endothelial hyperplasia)	Increased because of PG accumulation	Increased because of VSMC overgrowth	Increased because of VSMC overgrowth
Elastic fiber involvement	Yes	Yes	Yes	Yes
Wall thickness	Thinned	Increased	Increased	Increased
Involved layers	Intima/media/adventitia	Media > intima	Media	Intima
Calcium deposits	Yes	Yes	No	Yes
Inflammation	No	No	No	Yes

AD-HIES, Autosomal dominant hyper-IgE syndrome; *ELN*, elastin gene; *FBNI*, fibrillin gene; *IMT*, intima media thickness; *MRI*, magnetic resonance imaging; *PG*, proteoglycan.